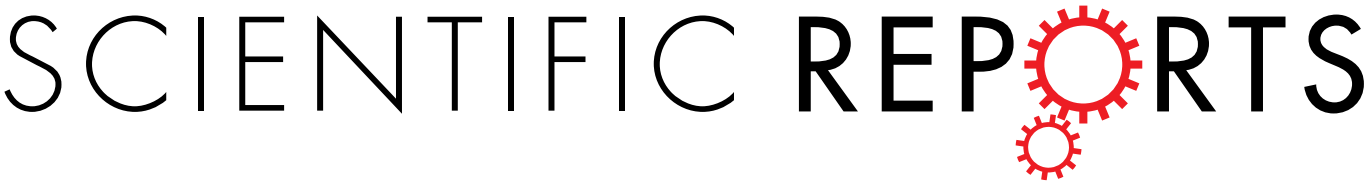

OPEN

Pressure induced superconductivity in the antiferromagnetic Dirac material $BaMnBi_2$

Received: 19 December 2016
Accepted: 6 April 2017
Published online: 09 May 2017

Huimin Chen[1], Lin Li[1], Qinqing Zhu[1], Jinhu Yang[1], Bin Chen[1], Qianhui Mao[2], Jianhua Du[2], Hangdong Wang[1,2] & Minghu Fang[2,3]

The so-called Dirac materials such as graphene and topological insulators are a new class of matter different from conventional metals and (doped) semiconductors. Superconductivity induced by doing or applying pressure in these systems may be unconventional, or host mysterious Majorana fermions. Here, we report a successfully observation of pressure-induced superconductivity in an antiferromagnetic Dirac material $BaMnBi_2$ with T_c of ~4 K at 2.6 GPa. Both the higher upper critical field, $\mu_0 H_{c2}(0) \sim 7$ Tesla, and the measured current independent of T_c precludes that superconductivity is ascribed to the Bi impurity. The similarity in $\rho_{ab}(B)$ linear behavior at high magnetic fields measured at 2 K both at ambient pressure (non-superconductivity) and 2.6 GPa (superconductivity, but at the normal state), as well as the smooth and similar change of resistivity with pressure measured at 7 K and 300 K in zero field, suggests that there may be no structure transition occurred below 2.6 GPa, and superconductivity observed here may emerge in the same phase with Dirac fermions. Our findings imply that $BaMnBi_2$ may provide another platform for studying SC mechanism in the system with Dirac fermions.

The so-called Dirac materials such as graphene and topological insulators (TIs), in which a linear energy dispersion similar to the spectrum of relativistic Dirac particles was found, are a new class of matter different from conventional metals and (doped) semiconductors[1], in which a quadratic dispersion was commonly observed. According to the Bardeen-Cooper-Schrieffer (BCS) theory in the weak-coupling limit, the low density of states (DOS) at the Fermi level for un-doped or lightly doped Dirac materials is usually harmful to superconductivity (SC) emerging in these materials. However, SC has been observed in many Dirac materials, such as the Cu-doped TI Bi_2Se_3[2–4], $Sn_{1-x}In_xTe$[5], as well as the pressurized TIs Bi_2Se_3[6], Bi_2Te_3[7] and Sb_2Te_3[8,9]. In the $Cu_xBi_2Se_3$ superconductor (its superconducting transition temperature, $T_c \sim 3.4$ K), the presence of a zero-bias conductance peak (ZBCP) in the point-contact spectra on its cleaved surface may give evidence for a topological SC[4]. The very recent results of the nuclear magnetic resonance (NMR) measurements[10] for $Cu_xBi_2Se_3$ established a spin-triplet SC in this compound. Especially, the topological superconductors are expected to host unusual Majorana fermions on its surface[11–13], which are peculiar in that the particles are their own antiparticles, and are originally conceived as mysterious neutrinos[14]. The realization of Majorana fermions in condensed matter is of significant interest because of their novelty as well as the potential for quantum computing[14]. Triggered by these researches, now searching for SC and exploring the nature of SC in various Dirac materials become a very hot field in the condensed matter physics.

$BaMnBi_2$[15] consists of a MnBi layer with edge-sharing $MnBi_4$ tetrahedrons and a two-dimensional (2D) Bi square net stacked with Ba atoms as shown in Fig. 1(a). As discussed by Park *et al.*[16] for the isostructural $SrMnBi_2$, the ionic Ba layers electronically separate the MnBi layers and the Bi square net because of the low electronegativity of Ba. In the $[MnBi]^-$ layer, Mn^{2+} has a half filled $3d^5$ configuration. The strong Hund coupling of Mn^{2+} leads to an antiferromagnetic ground state in MnBi layers[17]. Based on the first-principles calculations, angle-resolved photoelectron spectroscopy (ARPES) measurements[15,16,18–23], it has been confirmed that the Mn bands are placed away from the Fermi level (E_F), the states near E_F are dominated by the Bi states in the square net where the Dirac-like energy dispersion is seen at $k_0 = (0.208, 0.208)$. There are two identical Bi atoms per unit cell because

[1]Hangzhou Key Laboratory of Quantum Matter, Department of Physics, Hangzhou Normal University, Hangzhou, 310036, China. [2]Department of Physics, Zhejiang University, Hangzhou, 310027, China. [3]Collaborative Innovation Center of Advanced Microstructures, Nanjing, 210093, China. Correspondence and requests for materials should be addressed to H.W. (email: hdwang@hznu.edu.cn) or M.F. (email: mhfang@zju.edu.cn)

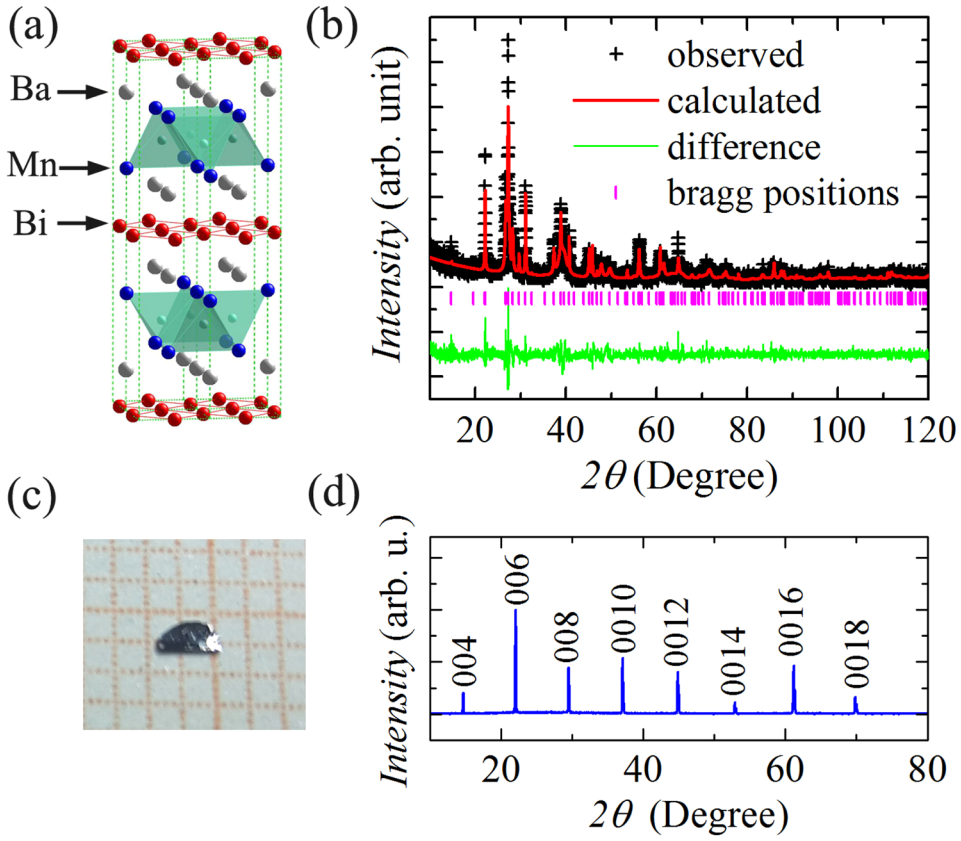

Figure 1. (**a**) Crystal structure of $BaMnBi_2$. (**b**) XRD pattern of powder obtained by grinding $BaMnBi_2$ crystals. Its Rietveld refinement is shown by the solid lines. (**c**) A photo of $BaMnBi_2$ crystal. (**d**) Single-crystal XRD pattern of $BaMnBi_2$.

Ba atoms below and above the square net result in unit cell doubling. This leads to folding of the dispersion Bi 6*p* bands and makes the two Bi $p_{x,y}$ bands cross each other. The Ba-Bi hybridization lifts the degeneracy of the folded bands except the momentum space along the Γ-*M* symmetry line, resulting in the formation of the Dirac cone. A small gap near the Dirac point appears due to the presence of the spin-orbital coupling (SOC). The magnetotransport properties, nonzero Berry phase, small cyclotron mass measurements[15] on $BaMnBi_2$ also confirm the presence of Dirac fermions in Bi square net. The quantum oscillations[15] in the Hall channel suggest the presence of both electron and hole pockets, whereas Dirac and parabolic states coexist at the E_F. On the other hand, the Dirac materials $AnMnBi_2$ (An = Ca, Sr, Ba) are suggested to be promising parent compounds for superconductivity, due to their striking similarity to the superconducting iron pnictides. Up to now, superconductivity has not been observed in these materials, although several authors suggested that chemical doping may introduce superconductivity in these systems[16,20]. Here, we report a successfully observation of pressure-induced superconductivity in an antiferromagnetic Dirac material $BaMnBi_2$ with T_c of ~4 K, at 2.6 GPa. Our findings imply that $BaMnBi_2$ may provide another platform for studying SC mechanism in the system with Dirac fermions.

Results and Discussion

We grew the $BaMnBi_2$ crystals using a self-flux method (see the method in details). The x-ray diffraction (XRD) pattern [see Fig. 1(b)] of $BaMnBi_2$ powder created by grinding pieces of crystals confirms its tetrahedral structure with space group *I*4/*mmm*, and its Rietveld refinement [see Fig. 1(b)] gives the lattice parameters of $a = 4.628(1)$ Å and $c = 24.092(4)$ Å, in consistent with the previous results reported by Li *et al.*[15]. Single crystal XRD pattern [see Fig. 1(d)] shows that the basal plane of a cleaved crystal is the crystallographic *ab*-plane. The energy-dispersive x-ray spectroscopy (EDX) results indicate that the crystals are rather homogenous and the determined average atomic ratios are Ba:Mn:Bi = 1.02:0.99:2.00 when fixing Bi stoichiometry to be 2, confirming the stoichiometry of $BaMnBi_2$.

The physical properties of $BaMnBi_2$ crystal are summarized in Fig. 2. The temperature dependence of the in-plane, ρ_{ab}, and out-plane, ρ_c, resistivity at ambient pressure is shown in Fig. 2(a). Both $\rho_{ab}(T)$ and $\rho_c(T)$ exhibit a metallic behavior. However, ρ_c is almost two orders of magnitude larger than ρ_{ab}, *i.e.* at 300 K $\rho_c/\rho_{ab} \approx 41$. The strong anisotropy in resistivity is consistent with its quasi-2D electronic structure in $BaMnBi_2$ as discussed above. Figure 2(b) shows $\rho_{ab}(T)$ curves at various magnetic fields. It is clear that the magnetic field induced metal-insulator transition occurs, such as, at 6 Tesla, its ρ_{ab} increases with decreasing temperature, and reaches a constant at the low temperatures, *i.e.* exhibiting a semiconductor-like behavior. Even at room temperature (300 K), there is also a large different in resistance at different magnetic fields, indicating that $BaMnBi_2$ exhibits

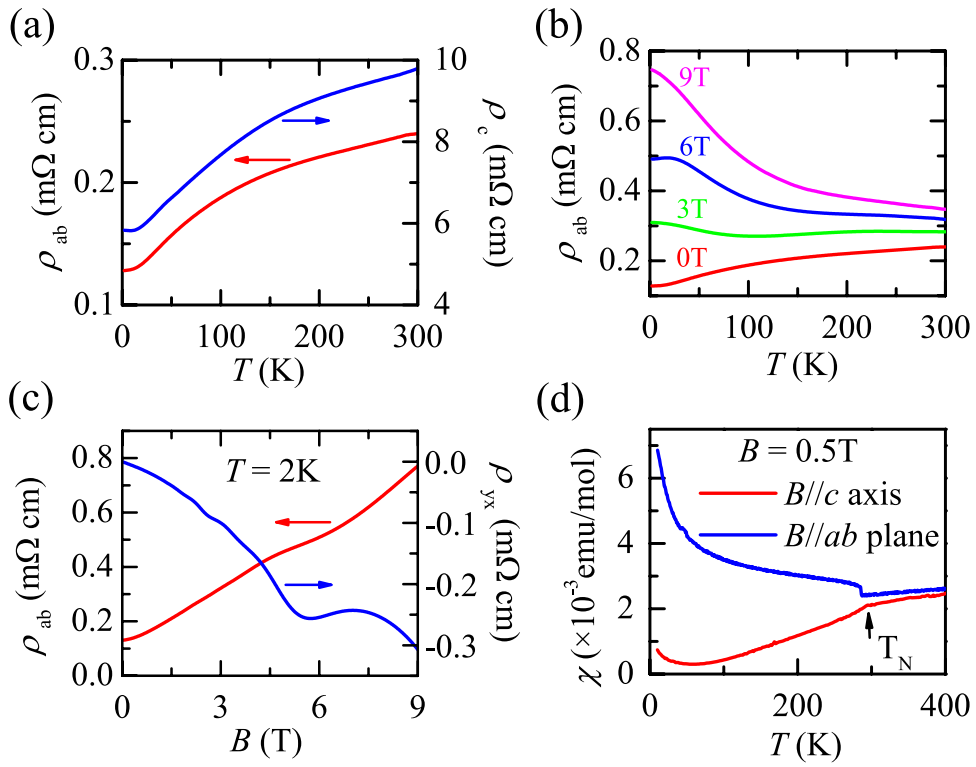

Figure 2. (**a**) Temperature dependence of the in-plane (ρ_{ab}) and out-plane (ρ_c) resistivity. (**b**) Temperature dependence of the ρ_{ab} under various fields. (**c**) ρ_{ab} and Hall resistivity (ρ_{yx}) as a function of the out-of plane magnetic field at $T = 2$ K. (**d**) Temperature dependence of the magnetic susceptibility with field parallel and perpendicular to c axis for $BaMnBi_2$ crystal.

a large magnetoresistance. Figure 2(c) shows the ρ_{ab} and Hall resistivity, ρ_{yx}, as a function of the out-of plane magnetic field at $T = 2$ K. Clear Shubnikov-deHaas (SdH) oscillations in both the $\rho_{ab}(B)$ and Hall resistivity $\rho_{yx}(B)$ are observed, indicating the presence of small fermi surface in $BaMnBi_2$. Figure 2(d) displays the temperature dependence of magnetic susceptibility, $\chi(T)$. At the Néel temperature, $T_N = 288$ K, an antiferromagnetic (AFM) transition was clearly observed. All these results are quite similar with that reported by Li *et al.*[15], also suggesting the existence of the Dirac fermions in our crystals. However, compared with their results, a major difference is found in Hall resistivity, which is negative, indicating that the electrons are dominant carriers in our crystals, which may origin from the slight shift of the E_F near the Dirac cone by a light electron-doping.

The key result of this work is shown in Fig. 3. The evolution of the normalized resistivity, $\rho_{ab}(T)/\rho_{ab}$ (300 K), as a function of temperature at various pressures for $BaMnBi_2$ crystal is shown in Fig. 3(a). It can be seen that the metallic behavior in $\rho_{ab}(T)$ at higher temperatures, *i.e.*, ρ_{ab} monotonously deceases with deceasing temperature, is robust to pressure. At T_N, no anomaly in $\rho_{ab}(T)$ due to AFM transition from the Mn^{2+} moments was observed under all the applied pressures, which is in consistent with the conduction in $BaMnBi_2$ determined by the Bi states in the square net as discussed above, therefore makes it impossible to figure out the pressure dependence of T_N by using only the resistance measurements. It is very interesting that a clear superconducting transition was observed at pressures above 2.4 GPa, even at 2.1 GPa a slight drop in ρ_{ab} can be distinguished. The definition of superconducting transition temperatures of onset, midpoint, and zero resistance, for 2.6 GPa data are shown in Fig. 3(c), and $T_c^{onset} = 4.13$ K, $T_c^{mid} = 3.97$ K and $T_c^{zero} = 3.69$ K were obtained. Compared with the data of 2.4 GPa, it should be pointed out that there are other two kinks in resistance for 2.6 GPa at $T = 5.86$ K and 6.81 K, respectively. The origin of these two kinks is not clear yet, however, we suggest that they may be associated with other two superconducting transitions, since they are smoothed out by the applied field. This result indicates that SC with higher T_c may emerges at higher pressures. At the same time, we plot the resistivity data at 2.6 GPa as a function of T^2 up to 30 K, as shown in the inset of Fig. 3(c), in which the good $\rho_{ab}(T) \sim T^2$ behavior above T_c indicates its fermi liquid ground state. In order to check whether the structure transition occurs by applying pressure, we plot the resistivity data at 300 K and 7 K as a function of pressure, as shown in Fig. 3(b). It can be seen that the resistivity deceases smoothly with increasing pressure. The smooth and similarity of ρ_{ab} changing with pressure at both temperatures may preclude the possibility of structure transition occurring below 2.6 GPa. However, further work is still needed to confirm this result.

About the origin of the superconductivity, we noted that the T_c for $BaMnBi_2$ is very close to that of Bi single crystal under high pressure[24,25]. To assure what has been observed in Fig. 3 is indeed a superconducting transition and to exclude the SC originating from Bi impurity, we further conducted the measurements at variant external magnetic field at 2.6 GPa. As shown in Fig. 4(a), with the increase of magnetic field, the superconducting transition temperature decreases, and the width of superconducting transition increases gradually from 0.4 K at zero

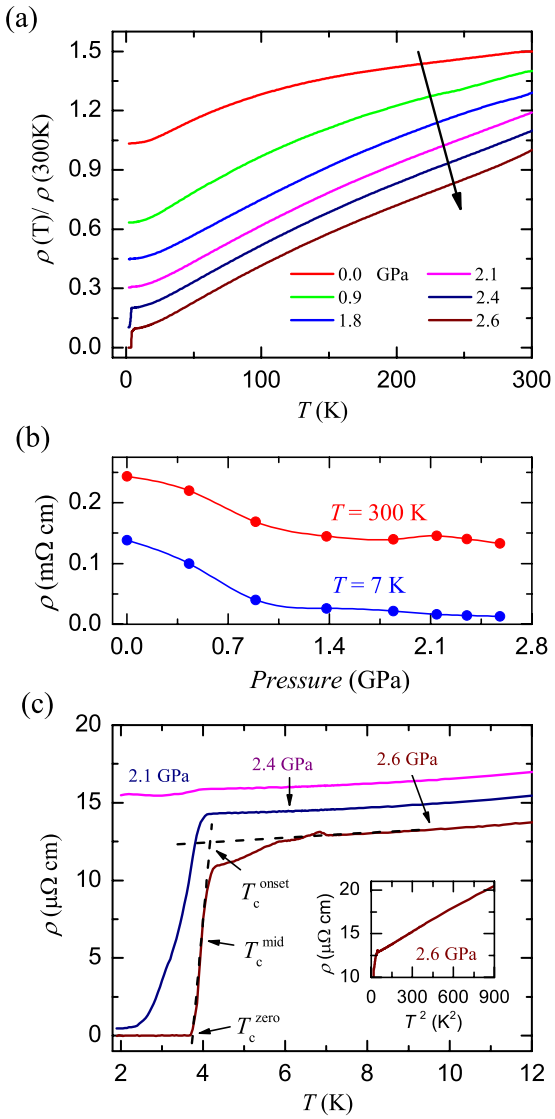

Figure 3. (**a**) Temperature dependence of the normalized in-plane resistivity, $\rho(T)/\rho(300\,K)$, for a $BaMnBi_2$ crystal under various pressures up to 2.6 GPa. Note that each subsequent data set is shifted upward by 0.1 for clarity. (**b**) Pressure dependence of ρ measured at 300 K and 7 K. (**c**) The low temperature $\rho(T)$ curves measured at various pressures. The criteria used to determine the onset, middle and zero temperatures for the superconducting transitions. Inset: ρ as a function of T^2 below 30 K under 2.6 GPa.

field to 1.2 K at 1 T. The upper critical field $\mu_0 H_{c2}$ as a function of T_c^{onset}, T_c^{mid}, and T_c^{zero} is plotted in Fig. 4(b), respectively. It can be seen that $\mu_0 H_{c2}(T)$ near T_c has a positive curvature, a characteristic of two band clean-limit type-II superconductors, like YNi_2B_2C, $LuNi_2B_2C$[26], MgB_2[27], or $TlNi_2Se_2$[28]. According to the Ginzburg-Landau theory, the zero temperature upper critical field $H_{c2}(0)$ can be estimated by using the formula $H_{c2}(T) = H_{c2}(0)(1-t^2)/(1+t^2)$, where t is the reduced temperature $t = T/T_c$. Using the T_c^{onset}, T_c^{mid}, and T_c^{zero}, the fitting result yields the value of $\mu_0 H_{c2}(0) = 7.0$, 4.6, and 2.4 Tesla, respectively. Compared with the critical field of Bi element under high pressure, these values are two orders of magnitude larger. Besides, we also carried out resistivity measurements with different applied currents, and no obvious difference in T_c was observed. So, we conclude that the observed SC is intrinsic to $BaMnBi_2$, and can't be ascribed to the Bi impurity.

In addition to the SC in $BaMnBi_2$ at high pressures, the large magnetoresistivity effect [see Fig. 4(a)] due to the presence of Dirac fermions is also survived. Figure 4(c) displays the ρ_{ab} at 2 K measured at both ambient and 2.6 GPa pressure, respectively, as a function of magnetic field, B. It can be seen that the ρ_{ab} measured at ambient pressure increases with increasing magnetic field, and exhibits a linear behavior at higher field, while $\rho_{ab}(B)$ measured at 2.6 GPa has a similar behavior as $B > 4$ Tesla (at the normal state). The similarity in $\rho_{ab}(B)$ behavior measured both at ambient pressure and 2.6 GPa in the high magnetic field range indicates that SC observed here emerges in the same phase with Dirac fermions. Therefore, we suspect that the Dirac fermions may preserve under high pressure and play an important role in the SC in $BaMnBi_2$. Our findings imply that $BaMnBi_2$ may provide another platform for studying SC mechanism in the system with Dirac fermions.

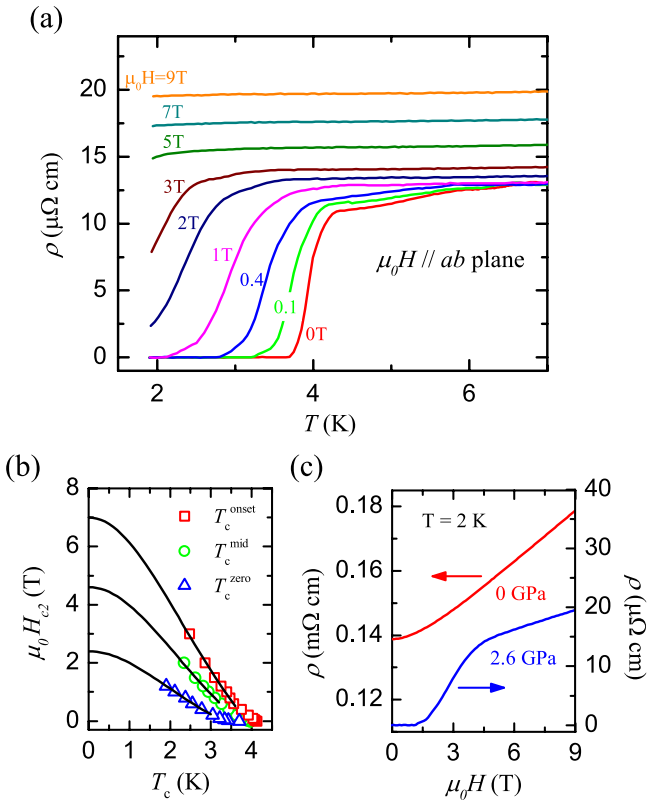

Figure 4. (**a**) Temperature dependence of the *ab*-plane resistivity measured at 2.6 GPa in magnetic fields up to 9 T for $BaMnBi_2$ crystal. (**b**) Upper critical field $\mu_0 H_{c2}$ *vs* T_c determined by using the superconducting transition temperatures in (**a**). (**c**) Magnetic field dependence of ρ measured at 2 K under ambient pressure and 2.6 GPa. The field is parallel to *ab*-plane.

Finally, we should point out that $BaMnBi_2$, as an AFM compound of Mn^{2+} $3d^5$ half-filled electrons with $T_N = 288$ K at ambient pressure, is expected to be a promising parent for SC. As we know, in the cuprates, Fe-pnictides, and heavy-fermion compounds, doping or applying a pressure can suppress the AFM order, then unconventional SC emerges. Here, although we can't figure out the pressure dependence of T_N by using only resistance measurements as discussed above, we suspect that the AFM order in $BaMnBi_2$ seems impossible to be suppressed by such low pressure ($\leq$2.6 GPa), just like the robust antiferromagnetism under high pressure in $(Ba_{0.61}K_{0.39})Mn_2Bi_2$[29], which contains the similar Mn_2Bi_2 layers. Taken this assumption, then the SC observed here should originate from the electrons in Bi square net, which host both Dirac and parabolic states. Therefore, SC in the pressurized $BaMnBi_2$ may coexist with the AFM order. It is urgently needed to figure out the relationship among SC, AFM and Dirac fermions, as well as the symmetry of Cooper pairs in this system in the near future.

In summary, we present resistivity measurements on the antiferromagnetic ($T_N = 288$ K) Dirac material $BaMnBi_2$ under various pressures up to 2.6 GPa. At T_N, no anomaly in $\rho_{ab}(T)$ due to AFM transition was observed, which makes it impossible to figure out the pressure dependence of T_N by using only the resistance measurements. $\rho_{ab}(T)$ shows a clear superconducting transition with $T_c \sim 4$ K at 2.4 GPa, but does not drop to zero. Under 2.6 GPa, a sharp superconducting transition with $T_c^{onset} = 4.13$ K, $T_c^{mid} = 3.97$ K and $T_c^{zero} = 3.69$ K was observed. Both the higher upper critical field, $\mu_0 H_{c2}(0) \sim 7$ Tesla, close to its Pauli limit $H_p = 1.84$ $T_c \approx 7.2$ T, and the measured current independent of T_c precludes that SC is ascribed to the Bi impurity. The similarity in $\rho_{ab}(B)$ linear behavior at high magnetic fields measured at 2 K both at ambient pressure and 2.6 GPa indicates that SC observed here would emerge in the same phase with Dirac fermions. Our findings imply that $BaMnBi_2$ may provide another platform for studying SC mechanism in the system with Dirac fermions.

Methods

High quality $BaMnBi_2$ single crystals were grown using self-flux method. First, Ba chunks, and Mn, Bi powders were mixed according to an appropriate stoichiometry and were put into alumina crucibles and sealed in an evacuated silica tube. The mixture was heated up to 850 °C and kept for 3 hours. Then the melting mixture was cooled down to 450 °C with a rate of 3 °C/h. Finally the furnace was cooled to room temperature after shutting down the power. The structure of single crystals was characterized by powder X-ray diffraction (XRD) measurement at ambient pressure. To avoid exposure to air, the sample was sealed using *N*-grease during the XRD data collecting. The elemental analysis was performed using an energy-dispersive x-ray spectroscopy (EDX) in a Zeiss Supra 55 scanning electron microscope. The measurements of resistivity under various hydrostatic pressures below 3 GPa, were carried out in the *QuantumDesign* Physical Properties Measurement System PPMS-9. The magnetic

susceptibility χ(T) was measured using the *QuantumDesign* MPMS-SQUID. Pressure was generated in a Teflon cup filled with Fluorinert FC-75, which was inserted into a nonmagnetic, piston-cylinder type, Be-Cu pressure cell with a core made of NiCrAl alloy. The pressure was determined at low temperature by monitoring the shift in the T_c of pure lead.

References

1. Wehling, T. O., Black-Schaffer, A. M. & Balatsky, A. V. Dirac materials. *Adv. phys.* **63**, 1–76, doi:10.1080/00018732.2014.927109 (2014).
2. Wray, L. A. *et al*. Observation of topological order in a superconducting doped topological insulator. *Nat. Phys.* **6**, 855–859, doi:10.1038/nphys1762 (2010).
3. Hor, Y. S. *et al*. Superconductivity in $Cu_xBi_2Se_3$ and its implications for pairing in the undoped topological insulator. *Phys. Rev. Lett.* **104**, 057001, doi:10.1103/PhysRevLett.104.057001 (2010).
4. Sasaki, S. *et al*. Topological superconductivity in $Cu_xBi_2Se_3$. *Phys. Rev. Lett.* **107**, 217001, doi:10.1103/PhysRevLett.107.217001 (2011).
5. Sasaki, S. *et al*. Odd-parity pairing and topological super-conductivity in a strongly spin-orbit coupled semiconduc-tor. *Phys. Rev. Lett.* **109**, 217004, doi:10.1103/PhysRevLett.109.217004 (2012).
6. Kirshenbaum, K. *et al*. Pressure-induced unconventional superconducting phase in the topological insulator Bi_2Se_3. *Phys. Rev. Lett.* **111**, 087001, doi:10.1103/PhysRevLett.111.087001 (2013).
7. Zhang, J. L. *et al*. Pressure-induced supercon-ductivity in topological parent compound Bi_2Te_3. *Proc. Natl. Acad. Sci. USA* **108**, 24–28, doi:10.1073/pnas.1014085108 (2011).
8. Zhu, J. *et al*. Superconductivity in topological insulator Sb_2Te_3 Induced by Pressure. *Sci. Rep.* **3**, 2016, doi:10.1038/srep02016 (2013).
9. Zhao, L. *et al*. Emergent surface superconductivity in the topological insulator Sb_2Te_3. *Nat. Commun.* **6**, 8279, doi:10.1038/ncomms9279 (2015).
10. Matano, K. *et al*. Spin-rotation symmetry breaking in the superconducting state of $Cu_xBi_2Se_3$. *Nature Phys.* **3781**, 067007–854, doi:10.1038/nphys3781 (2016).
11. Qi, X.-L. & Zhang, S. C. Topological insulators and super-conductors. *Rev. Mod. Phys.* **83**, 1057–1110, doi:10.1103/RevModPhys.83.1057 (2011).
12. Schnyder, A. P. *et al*. Classification of topological insulators and superconductors in three spatial dimensions. *Phys. Rev. B* **78**, 195125, doi:10.1103/PhysRevB.78.195125 (2008).
13. Sato, M. Topological odd-parity superconductors. *Phys. Rev. B* **81**, 220504(R), doi:10.1103/PhysRevB.81.220504 (2010).
14. Wilczek, F. Majorana returns. *Nature Phys.* **5**, 614–618, doi:10.1038/nphys1380 (2009).
15. Li, L. J. *et al*. Electron-hole asymmetry, Dirac fermions and quantum magnetoresistance in $BaMnBi_2$. *Phys. Rev. B* **93**, 115141, doi:10.1103/PhysRevB.93.115141 (2016).
16. Park, J. *et al*. Anisotropic Dirac fermions in a Bi square net of $SrMnBi_2$. *Phys. Rev. Lett.* **107**, 126402, doi:10.1103/PhysRevLett.107.126402 (2011).
17. Guo, Y. *et al*. Coupling of magnetic order to planar Bi electrons in the anisotropic Dirac metals $AMnBi_2$ (A = Sr, Ca). *Phys. Rev. B* **90**, 075120, doi:10.1103/PhysRevB.90.075120 (2014).
18. Wang, K. F. *et al*. Quantum transport of two-dimensional Dirac fermions in $SrMnBi2_2$. *Phys. Rev. B* **84**, 220401, doi:10.1103/PhysRevB.84.220401 (2011).
19. Wang, K. F. *et al*. Two-dimensional Dirac fermions and quantum magnetoresistance in $CaMnBi_2$. *Phys. Rev. B* **85**, 041101, doi:10.1103/PhysRevB.85.041101 (2012).
20. Wang, J. K. *et al*. Layered transition-metal pnictide $SrMnBi_2$ with metallic blocking layer. *Phys. Rev. B* **84**, 064428, doi:10.1103/PhysRevB.84.064428 (2011).
21. Feng, Y. *et al*. Strong anisotropy of Dirac cones in $SrMnBi_2$ and $CaMnBi_2$ Revealed by angle-resolved photoemission spectroscopy. *Sci. Rep.* **4**, 5385, doi:10.1038/srep05385 (2014).
22. Jo, Y. J. *et al*. Valley-polarized interlayer conduction of anisotropic Dirac fermions in $SrMnBi_2$. *Phys. Rev. Lett.* **113**, 156602, doi:10.1103/PhysRevLett.113.156602 (2014).
23. He, J. B., Wang, D. M. & Chen, G. F. Giant magnetoresistance in layered manganese pnictide $CaMnBi_2$. *Appl. Phys. Lett.* **100**, 112405, doi:10.1063/1.3694760 (2012).
24. Brandt, N. B. & Ginzburg, N. I. Critical fields of the crystalline modifications BI-II and BI-III. *Sov. Phys. JETP* **17**, 326–1357 (1963).
25. Li, Y. F., Wang, E. Y., Zhu, X. Y. & Wen, H. H. Pressure induced superconductivity in Bi single crystals. *Phys. Rev. B* **95**, 024510, doi:10.1103/PhysRevB.95.024510 (2017).
26. Freudenberger, J. *et al*. Superconductivity and disorder in $Y_xLu_{1-x}Ni_2B_2C$. *Phys. C* **306**, 1 (1998).
27. Muller, K. H. *et al*. The upper critical field in supercon-ducting MgB_2. *J. Alloys Compd.* **322**, L10–L13, doi:10.1016/S0925-8388(01)01197-5 (2001).
28. Wang, H. D. *et al*. Multiband Superconductivity of Heavy Electrons in a $TlNi_2Se_2$ Single Crystal. *Phys. Rev. Lett.* **111**, 207001, doi:10.1103/PhysRevLett.111.207001 (2013).
29. Gu, D. C. *et al*. Robust antiferromagnetism prevent- ing superconductivity in pressurized $(Ba_{0.61}K_{0.39})Mn_2Bi_2$. *Sci. Rep.* **4**, 7342 (2014).

Acknowledgements

We thank Zhi Ren and Chao Cao for helpful discussions. This work is supported by the National Basic Research Program of China under grant No. 2016YFA0300402, 2015CB921004, and 2012CB821404, the Nature Science Foundation of China (Grant No. 11374261, and 11204059), and Zhejiang Provincial Natural Science Foundation of China (Grant No. LY14A040007), and the Fundamental Research Funds for the Central Universities of China.

Author Contributions

Minghu Fang and Hangdong Wang designed the study, analysed data and wrote the paper. Hangdong Wang and Huimin Chen synthesized the sample; Lin Li and Huimin Chen did the transport measurements under high pressure; Qianhui Mao collected, processed and refined the X-ray data; Jinhu Yang and Bin Chen did the magnetic susceptibility measurement; Qinqing Zhu and Jinhua Du did the EDS analysis; Huimin Chen and Lin Li contributed equally to the study; All authors discussed the results and commented on the manuscript.

Additional Information

Competing Interests: The authors declare that they have no competing interests.

Publisher's note: Springer Nature remains neutral with regard to jurisdictional claims in published maps and institutional affiliations.